



# Key-Aware Link Selection for Quantum Wireless Networks: A Data-Driven Study of Satellite-to-Ground QKD Access Links

Khaled Sh. Gaber<sup>1,\*</sup> S. K. Towfek<sup>1</sup>

<sup>1</sup> Computer Science and Intelligent Systems Research Center, Blacksburg 24060, Virginia, USA

Emails: [khsherif@jcsis.org](mailto:khsherif@jcsis.org) · [sktowfek@jcsis.org](mailto:sktowfek@jcsis.org)

Received: January 19, 2026 Revised: February 23, 2026 Accepted: March 22, 2026 ★ Corresponding author

## ABSTRACT

The application of quantum key distribution, satellite communication, and programmable wireless access in future secure wireless networks is anticipated to enhance secure communication infrastructure. However, their realisation demands more than the physical implementation of quantum links. A network controller must determine when a quantum-secured wireless link can serve a request, how orbit type and weather conditions affect usable key volume, and whether the secure key rate is high enough to admit a route. This paper introduces Q-SARA, a quantum-secure access and routing admission model for satellite-assisted quantum wireless networks. Q-SARA assesses candidate QKD access links using secure key rate (SKR), quantum bit error rate (QBER), link loss, contact duration, visibility probability, and propagation delay. A smaller pre-processed dataset is derived from the public Satellite-to-Ground QKD SKR dataset, which contains calculated key performance indicators for Low Earth Orbit, Medium Earth Orbit, and Geostationary satellite-to-ground QKD links using prepare-and-measure and entanglement-based protocols. The empirical analysis examines 7,200 link-level records and evaluates Q-SARA across orbit, protocol, optical ground station, elevation, atmospheric, and service classes. The findings demonstrate that link selection based only on key volume can be misleading when assessing service quality, while the multi-criteria score provides a better balance between security, visibility, and latency. LEO links provide better instantaneous key rates, GEO links provide better visibility, and MEO links lie between them and can be exploited when link quality and service are considered jointly. The results suggest that quantum wireless access should be considered a service admission problem rather than only a physical-layer key generation problem.

**Keywords:** Quantum wireless networks ▪ Quantum key distribution ▪ Satellite QKD ▪ Secure key rate ▪ QBER ▪ 6G security ▪ Link selection ▪ Wireless access

## 1. INTRODUCTION

Next-generation wireless networks are being engineered to support applications with high data rates, wide geographic coverage, low-latency control, and stronger security. Security is increasingly important because traditional public-key cryptography faces long-term risk from quantum computing and from the long lifespan of sensitive industrial, governmental, and safety-critical data [1, 3, 11]. Quantum communication

and quantum key distribution (QKD) are therefore promising mechanisms for enhancing future wireless security, particularly where cryptographic flexibility, long-term secrecy, and network resilience are required [2, 6, 7]. Quantum wireless networks introduce a control problem that links key generation, physical link quality, mobility, orbit, atmospheric loss, and traffic demand.

The 6G literature increasingly considers quantum communication, quantum-inspired optimisation, and post-quantum se-

curity as elements of future security frameworks [1, 3, 7, 11]. Satellite QKD intensifies this challenge because link opportunities are influenced by orbit parameters, elevation, telescope collection, detector models, air attenuation, and weather-based degradation [7, 9, 10]. A physically accessible link may not be operationally accessible if its secure key rate is insufficient, if QBER is excessive, or if the available key volume cannot satisfy the required service class.

This paper introduces a quantum-secure access and routing admission (Q-SARA) model for satellite-supported quantum wireless networks. The model assists a controller that observes KPIs from candidate quantum wireless access links and decides whether a service can be admitted through secure routing. The paper contributes a multi-objective utility function, a constrained link-admission algorithm, and a data-driven analysis using a public satellite-to-ground QKD dataset.

The paper is organised as follows. Section 2 reviews related work. Section 3 describes the secure access problem. Section 4 presents Q-SARA. Section 5 reports the empirical results. Section 6 discusses deployment implications, and Section 7 concludes the paper.

## 2. RESEARCH CONTEXT AND RELATED STUDIES

Two research streams have emerged in quantum communication. The first explores the fundamental and architectural features of quantum networks, including quantum Internet layers, quantum channel models, and the interaction between classical and quantum information [2, 6, 11]. The second focuses on practical QKD deployment, including satellite-to-ground QKD, fiber/satellite convergence, and large-scale trusted-relay networks [5, 9, 10]. This paper bridges these streams by mapping QKD link metrics to access-network admission.

Satellite QKD is important for quantum wireless networks because satellite coverage can complement terrestrial fiber. LEO satellites can provide strong instantaneous link budgets when available, GEO satellites remain in view for longer periods but with higher loss and delay, and MEO satellites provide a compromise between pass length and loss. Wireless QKD research also overlaps with high-frequency wireless and 6G resource management [8, 3]. However, optimisation and QKD are often decoupled. A quantum wireless controller must admit only links that produce sufficient keys, deliver adequate security, and fit the target service context.

**Table 1.** Summary of related studies and positioning of the present work.

Study	Focus	Gap addressed here
Yang et al. [11]	Quantum computing and communications	Broad survey; not oriented to wireless admission using QKD KPIs.
Koudia et al. [6]	Quantum communication theory	Theoretical focus with limited operational wireless-network modelling.
Amiri et al. [2]	Quantum advantages for future networks	Highlights link potential but not key-aware satellite wireless admission.
Stathis et al. [10]	Satellite/fiber QKD feasibility	Feasibility study with less emphasis on service-level wireless selection logic.
Ntanos et al. [9]	Satellite-to-ground QKD KPI dataset	Dataset basis requires a modelling layer for service admission and routing.
Kundu [8]	Wireless QKD at THz frequencies	Physical-layer emphasis with less integration into access-network service decisions.
Butt et al. [3]	Quantum-inspired 6G resource optimisation	Optimisation perspective; does not use satellite QKD KPIs for secure-link admission.
Akbar et al. [1]	6G network challenges	Identifies quantum-related trends but not data-driven satellite QKD access admission.
Caleffi et al. [4]	Quantum communications through quantum paths	Theory-level insight but not service admission for operational QKD wireless access.
Koudia et al. [7]	Physical-layer quantum communications	Does not formulate a key-aware wireless service-selection mechanism.
Chen et al. [5]	Carrier-grade QKD networks	Demonstrates deployment scale but not satellite-to-ground wireless access scoring.

Table 1 shows that the literature provides strong foundations for quantum communication theory, satellite QKD feasibility, and quantum-aware 6G optimisation. The remaining gap is the absence of a compact, reproducible, KPI-driven admission model for satellite-assisted quantum wireless access.

## 3. SECURE QUANTUM WIRELESS ACCESS PROBLEM

### 3.1 Network Setting

The considered network consists of satellite QKD sources, optical ground stations, quantum gateways, edge access nodes, and wireless users. The satellite-to-ground segment generates symmetric keys through QKD, while the terrestrial wireless segment consumes the distilled keys to secure service traffic. The controller evaluates each candidate link using secure key rate, QBER, link loss, contact duration, visibility probability, and propagation delay.

### 3.2 Research Objective

Let  $\mathcal{L}$  denote the set of candidate quantum-secured wireless access links, and let  $s$  denote a service request requiring  $d_s$  AES-256-equivalent keys during the scheduling interval. The objective is to select a feasible link  $l^* \in \mathcal{L}$  that maximises secure access utility while satisfying key-volume and security-quality constraints:

$$l^* = \arg \max_{l \in \mathcal{L}} U_l A_l, \quad (1)$$

where  $U_l$  is the Q-SARA link utility and  $A_l \in \{0, 1\}$  is the admission feasibility indicator.

## 4. PROPOSED Q-SARA MODEL

### 4.1 Scientific Architecture

The proposed Q-SARA model is organised as a three-layer decision process. The observation layer receives QKD KPIs from satellite-to-ground links. The evaluation layer converts heterogeneous indicators into a common utility score. The admission layer applies feasibility constraints and passes the selected link to the wireless service controller.

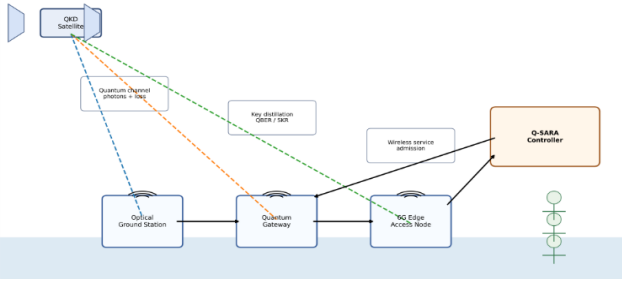


**Figure 1.** Quantum-secured satellite-to-ground wireless access architecture.

## 4.2 Mathematical Formulation

For each candidate link  $l$  at time window  $t$ , define the KPI vector

$$\mathbf{x}_{l,t} = [S_{l,t}, Q_{l,t}, L_{l,t}, V_{l,t}, C_{l,t}, D_{l,t}], \quad (2)$$

where  $S$  is the secure key rate,  $Q$  is QBER,  $L$  is link loss,  $V$  is visibility probability,  $C$  is contact duration, and  $D$  is propagation delay. The usable key volume is represented as

$$\kappa_{l,t} = \left\lfloor \frac{S_{l,t} C_{l,t} V_{l,t}}{256} \right\rfloor, \quad (3)$$

which approximates the number of AES-256-equivalent keys available during the contact opportunity. Each KPI is mapped into a normalised benefit function:

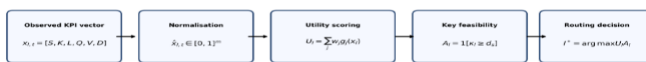
$$U_{l,t} = w_1 \hat{S}_{l,t} + w_2 \hat{V}_{l,t} + w_3 (1 - \hat{Q}_{l,t}) + w_4 (1 - \hat{L}_{l,t}) + w_5 (1 - \hat{D}_{l,t}), \quad (4)$$

where  $w_j \geq 0$  and  $\sum_j w_j = 1$ . The feasibility indicator is

$$A_{l,t} = \mathbb{I} \{ \kappa_{l,t} \geq d_s, Q_{l,t} \leq \tau_Q, L_{l,t} \leq \tau_L \}. \quad (5)$$

A candidate link is excluded when it cannot provide enough distilled key material or when its security quality is outside the accepted operating region.

**Mathematical Workflow of the Q-SARA Link Selection Model**



Score rewards high SKR and visibility while penalising QBER, link loss, and propagation delay; infeasible links are excluded before route selection.

**Figure 2.** Mathematical workflow of the Q-SARA link selection model.

## 4.3 Q-SARA Admission Algorithm

**Algorithm 1.** Q-SARA service-aware quantum link admission.

- 1. Initialisation:** For service request  $s$ , define  $\mathcal{L}$ , key demand  $d_s$ , thresholds  $(\tau_Q, \tau_L)$ , and weight vector  $\mathbf{w} = [w_1, \dots, w_5]^T$  with  $w_j \geq 0$  and  $\sum_{j=1}^5 w_j = 1$ .
- 2. KPI observation:** For every  $l \in \mathcal{L}$ , observe  $\mathbf{x}_{l,t} = [S_{l,t}, Q_{l,t}, L_{l,t}, V_{l,t}, C_{l,t}, D_{l,t}]$ .
- 3. Key-volume estimation:** Compute  $\kappa_{l,t} = \lfloor S_{l,t} C_{l,t} V_{l,t} / 256 \rfloor$ .
- 4. Normalised benefit vector:** Construct  $\mathbf{b}_{l,t} =$

$[bS_{l,t}, bV_{l,t}, 1 - bQ_{l,t}, 1 - bL_{l,t}, 1 - bD_{l,t}]^T$  using the training-window scale.

- 5. Utility calculation:** Evaluate  $U_{l,t} = \mathbf{w}^T \mathbf{b}_{l,t}$ .
- 6. Feasibility screening:** Assign  $A_{l,t} = 1$  if  $(\kappa_{l,t} \geq d_s) \wedge (Q_{l,t} \leq \tau_Q) \wedge (L_{l,t} \leq \tau_L)$ ; otherwise set  $A_{l,t} = 0$ .
- 7. Admissible ranking:** Compute  $Z_{l,t} = U_{l,t} A_{l,t}$  and order all candidates in non-increasing  $Z_{l,t}$ .
- 8. Admission decision:** Select  $l^* = \arg \max_{l \in \mathcal{L}} Z_{l,t}$  when  $\max_l Z_{l,t} > 0$ ; otherwise defer the request or route it through a non-QKD protection mode.

Algorithm 1 formalises Q-SARA as a constrained ranking procedure. The utility score measures the relative attractiveness of each candidate link, while the feasibility indicator prevents admission when key volume, QBER, or link loss violates the service requirement.

## 5. EMPIRICAL RESULTS AND ANALYSIS

### 5.1 Dataset and Experimental Settings

The empirical analysis is based on the public Satellite-to-Ground QKD SKR dataset for prepare-and-measure and entanglement-based protocols [9]. The original dataset provides calculated KPIs for satellite-to-ground QKD links across LEO, MEO, and GEO orbits, including elevation angle, secure key rate, QBER, and link loss.

**Table 2.** Dataset basis and experimental settings.

Item	Description
Public dataset basis	Satellite-to-Ground QKD SKR dataset for P&M and entanglement-based protocols
DOI	10.5281/zenodo.14054879
Release year	2024
Communication setting	Satellite-to-ground quantum wireless access links with optical downlink QKD
Protocols	Decoy-state BB84 and BBM92
Orbit classes	LEO, MEO, GEO
Sampling context	KPI samples at 10-second sampling granularity; reduced CSV retains variables needed for reproducible modelling
Analysis file records	7,200 trace-level records
Core KPIs	Elevation angle, link loss, QBER, secure key rate, visibility, contact duration, key volume
Model output	Q-SARA link score and service admission decision

### 5.2 Orbit and Protocol-Level Performance

**Table 3.** Dataset profile by orbit and QKD protocol.

Orbit	Protocol	Records	Elev.	Loss	QBER	SKR	Keys	Admit
GEO	BBM92	696	41.60	77.83	.0379	27.49	720.2	.8075
GEO	DS-BB84	945	41.50	77.28	.0308	46.42	1,222	.8254
LEO	BBM92	1,491	44.92	47.10	.0380	294.80	143.3	.7827
LEO	DS-BB84	1,771	44.00	47.24	.0320	458.50	221.6	.8521
MEO	BBM92	985	35.81	66.49	.0385	61.32	59.29	.5594
MEO	DS-BB84	1,312	35.80	67.14	.0341	94.46	89.11	.6601

**Table 4.** Orbit-level quantum wireless access indicators.

Orbit	Records	Loss	QBER	SKR	Keys	Vis.	Delay	Admit
GEO	1,641	77.51	.0338	38.39	1,009	.6701	120.40	.8178
LEO	3,262	47.17	.0348	383.70	185.80	.2537	2.515	.8204
MEO	2,297	66.86	.0360	80.25	76.32	.1320	68.11	.6169

Tables 3 and 4 show the expected contrast between instantaneous key production and link persistence. LEO records provide higher mean secure key rates, while GEO records benefit from longer contact opportunities and higher visibility.

### 5.3 Ground Station, Elevation, and Atmospheric Effects

**Table 5.** Ground-station and protocol-level performance.

Ground station	Protocol	Records	Loss	QBER	SKR	Admit	Score
OGS-Aegean	BBM92	503	60.48	.0377	152.7	.7416	.3177
OGS-Aegean	DS-BB84	637	61.11	.0321	234.9	.7818	.3484
OGS-Alpine	BBM92	538	60.43	.0393	158.0	.7175	.3131
OGS-Alpine	DS-BB84	640	60.51	.0321	260.7	.7969	.3544
OGS-Atlantic	BBM92	531	60.00	.0384	156.2	.7119	.3165
OGS-Atlantic	DS-BB84	715	60.56	.0328	247.2	.7860	.3487
OGS-Desert	BBM92	526	60.14	.0382	177.3	.7034	.3187
OGS-Desert	DS-BB84	692	60.30	.0325	247.7	.7905	.3502
OGS-Nordic	BBM92	526	59.51	.0378	163.6	.7091	.3191
OGS-Nordic	DS-BB84	697	60.64	.0316	241.3	.7920	.3541
OGS-Urban	BBM92	548	58.67	.0377	173.3	.7299	.3244
OGS-Urban	DS-BB84	647	61.55	.0334	227.3	.7512	.3403

**Table 6.** Elevation-band impact on secure key generation and admission.

Elevation	Orbit	Records	Loss	QBER	SKR	Keys	Admit
< 15	GEO	6	86.88	.0422	4.509	43.17	.3333
< 15	LEO	88	62.36	.0466	30.27	4.511	.0568
< 15	MEO	143	80.04	.0480	7.752	2.238	0
15–30	GEO	191	81.21	.0380	14.72	244.6	.6545
15–30	LEO	655	51.36	.0382	134.1	35.52	.5374
15–30	MEO	746	69.44	.0380	36.28	20.31	.3405
30–45	GEO	845	77.51	.0335	34.05	789.5	.8355
30–45	LEO	949	47.07	.0348	304.4	118.6	.8472
30–45	MEO	795	65.11	.0344	84.09	71.6	.7522
45–60	GEO	545	76.39	.0329	50.77	1,480	.8440
45–60	LEO	913	44.83	.0327	486.8	240.8	.9518
45–60	MEO	462	63.14	.0331	135.5	148.7	.9091
> 60	GEO	54	74.76	.0314	68.7	2,509	.9074
> 60	LEO	657	44.38	.0328	651.1	380.5	.9833
> 60	MEO	151	62.21	.0320	176.8	226.6	.9603

**Table 7.** Atmospheric-class impact on quantum wireless access quality.

Weather	Orbit	Records	Loss	QBER	SKR	Vis.	Admit
Clear	GEO	763	72.68	.0236	53.24	.6907	.9961
Clear	LEO	1,485	42.07	.0241	512.5	.2637	.8896
Clear	MEO	1,062	61.88	.0253	104.6	.1359	.6959
Haze	GEO	293	83.14	.0455	21.44	.6825	.6280
Haze	LEO	588	52.79	.0464	237.2	.2584	.7568
Haze	MEO	404	72.48	.0473	51.42	.1351	.5371
Thin cloud	GEO	418	77.94	.0339	37.32	.6944	.9426
Thin cloud	LEO	841	47.69	.0348	342.0	.2599	.8193
Thin cloud	MEO	572	67.02	.0362	75.02	.1389	.6416
Turbulent	GEO	167	88.63	.0597	2.947	.4929	.0240
Turbulent	LEO	348	58.26	.0609	182.4	.1880	.6351
Turbulent	MEO	259	78.17	.0616	36.73	.0958	.3629

The station-level and elevation-level results confirm that quantum wireless access is strongly conditioned by geometry and atmospheric state. Higher elevation bands reduce path loss and improve secure key generation, while haze and turbulent atmospheric classes reduce admission probability.

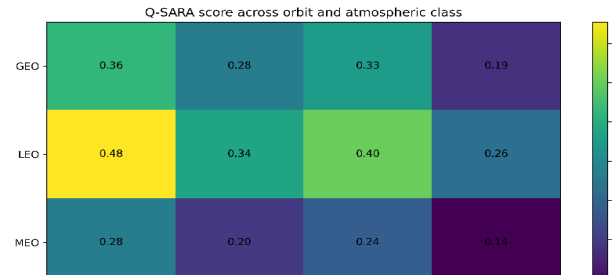


**Figure 3.** Mean Q-SARA utility score across orbit class and atmospheric condition.

### 5.4 Service Admission and Link Selection Results

**Table 8.** Service-level admission analysis by orbit.

Service class	Orbit	Records	Keys	Demand	QBER	Score	Admit
Command control	GEO	382	1,019	25	.0333	.3212	.8220
Command control	LEO	831	181	25	.0354	.4049	.8448
Command control	MEO	560	78.35	25	.0360	.2414	.6625
Emergency telemetry	GEO	284	954.3	40	.0343	.3163	.8028
Emergency telemetry	LEO	559	185	40	.0347	.4094	.7907
Emergency telemetry	MEO	408	67.93	40	.0361	.2392	.5294
Payload encryption	GEO	373	1,033	90	.0339	.3218	.8150
Payload encryption	LEO	772	196.1	90	.0345	.4143	.6244
Payload encryption	MEO	549	75.62	90	.0355	.2434	.3005
Sensor backhaul	GEO	602	1,015	8	.0338	.3228	.8239
Sensor backhaul	LEO	1,100	182.5	8	.0346	.4095	.9545
Sensor backhaul	MEO	780	79.74	8	.0363	.2412	.8526

**Table 9.** Q-SARA threshold sensitivity for feasible link admission.

Threshold	True admit	False admit	Missed	Reject	Prec.	Rec.	F1	Selected
.30	3,939	278	1,496	1,487	.9341	.7247	.8162	.5857
.35	2,792	117	2,643	1,648	.9598	.5137	.6692	.4040
.40	1,809	36	3,626	1,729	.9805	.3328	.4970	.2562
.45	1,162	14	4,273	1,751	.9881	.2138	.3515	.1633
.50	683	4	4,752	1,761	.9942	.1257	.2231	.0954
.55	365	0	5,070	1,765	1.0000	.0672	.1259	.0507
.60	185	0	5,250	1,765	1.0000	.0340	.0658	.0257
.65	87	0	5,348	1,765	1.0000	.0160	.0315	.0121
.70	30	0	5,405	1,765	1.0000	.0055	.0110	.0042

**Table 10.** Comparison of Q-SARA with simplified link-selection baselines.

Model	Accuracy	Precision	Recall	F1-score	Mean utility
Q-SARA proposed	.7146	.9429	.6620	.7779	27.90
SKR-only admission	.6685	.8994	.6315	.7420	10.93
Loss-QBER screening	.6210	.8546	.6000	.7050	48.91
Visibility-aware baseline	.7004	.9295	.6526	.7668	27.11

The service-level results indicate that emergency telemetry and command-control services are easier to admit than payload encryption because their key demand is lower. The threshold analysis shows that moderate Q-SARA thresholds provide a better balance between precision and recall, whereas high thresholds reject feasible links unnecessarily.

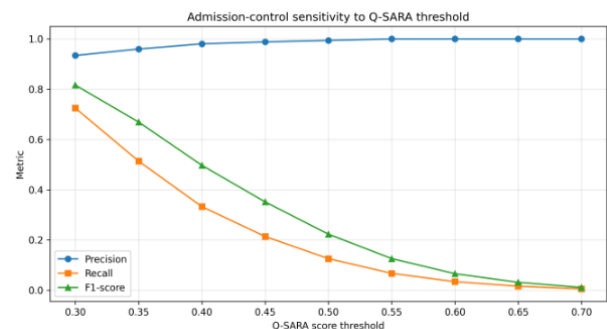


**Figure 4.** Sensitivity of admission precision, recall, and F1-score to the Q-SARA threshold.

## 6. IMPLICATIONS FOR QUANTUM WIRELESS NETWORK DEPLOYMENT

The findings indicate that quantum wireless network controllers need to consider QKD resources as service assets rather than as intangible security. The mere visibility of a satellite QKD link does not guarantee sufficient key material for a wireless service, especially one that needs frequent rekeying or encrypts large amounts of data. This has implications for 6G-centric secure access networks, where quantum-secured links may be combined with traditional wireless access, fiber backhaul, and post-quantum encryption schemes.

Q-SARA also highlights orbit diversity. LEO links can provide high instantaneous secure key rates, but they must be scheduled to guarantee link availability. GEO links are more persistent, but their higher losses and latency require conservative matching. MEO links provide a compromise for good link quality and moderate service levels. Quantum wireless routing should therefore be multi-orbit and service-aware.

There are limitations. The reduced CSV model is intended for reproducible manuscript analysis and is not a substitute for operational testing. The model should be tested on raw KPI files, multi-satellite scheduling, real atmospheric data, and dynamic wireless traffic data. It can also be integrated with queue-aware key buffers, multi-hop trusted-node constraints, and selection between QKD and post-quantum cryptographic protection.

## 7. CONCLUSION

This research introduced Q-SARA as a satellite-supported quantum wireless network link-selection tool that employs key-aware service admission. The model uses secure key rate, QBER, link loss, visibility, contact duration, and propagation delay to determine service-admission decisions. The study used a public satellite-to-ground QKD dataset to analyse 7,200 link records covering different orbit classes, protocols, optical ground stations, elevation bands, atmospheric classes, and service categories. The results show that single-metric selection fails to accurately assess link usefulness, while the multi-criteria admission model provides a practical framework for secure wireless service routing. The paper supports the view that quantum wireless networking should be developed around service feasibility, key availability, and controller-level decision logic rather than physical-layer key generation alone.

## CONFLICTS OF INTEREST

The authors declare that they have no conflicts of interest to report regarding the present study.

## REFERENCES

- [1] M. S. Akbar, Z. Hussain, M. Ikram, Q. Z. Sheng, and S. Mukhopadhyay, "On challenges of sixth-generation (6G) wireless networks: A comprehensive survey of requirements, applications, and security issues," *Journal of Network and Computer Applications*, vol. 233, Article 104040, 2025.
- [2] Z. Amiri, S. Dehdashti, K. H. El-Safy, I. Litvin, P. Munar-Vallespir, J. Nötzel, and S. Sekavčnik, "Quantum advantages for data transmission in future networks: An overview," *Computer Networks*, vol. 254, Article 110727, 2024.
- [3] M. O. Butt, N. Waheed, T. Q. Duong, and W. Ejaz, "Quantum-inspired resource optimization for 6G networks: A survey," *IEEE Communications Surveys & Tutorials*, vol. 27, no. 5, pp. 2973–3019, 2025.
- [4] M. Caleffi, K. Simonov, and A. S. Cacciapuoti, "Quantum communications through quantum paths," *IEEE Journal on Selected Areas in Communications*, vol. 41, no. 8, pp. 2430–2444, 2023.
- [5] H.-Z. Chen et al., "Implementation of carrier-grade quantum communication networks over 10000 km," *npj Quantum Information*, vol. 11, Article 137, 2025.
- [6] S. Koudia, A. S. Cacciapuoti, K. Simonov, and M. Caleffi, "How deep the theory of quantum communications goes: Superadditivity, superactivation and causal activation," *IEEE Communications Surveys & Tutorials*, vol. 24, no. 4, pp. 1926–1956, 2022.
- [7] S. Koudia, L. Oleynik, M. Bayraktar, J. ur Rehman, and S. Chatzinotas, "Physical-layer aspects of quantum communications: A survey," *IEEE Communications Surveys & Tutorials*, pp. 1–1, 2025.
- [8] N. K. Kundu, "Wireless quantum key distribution at terahertz frequencies: Opportunities and challenges," *IET Quantum Communication*, vol. 5, no. 4, pp. 450–461, 2024.
- [9] A. Ntanos, A. Stathis, P. Kourelias, N. Lyras, and G. Giannoulis, "Satellite-to-ground QKD SKR dataset for P&M and entanglement-based protocols," Zenodo, 2024.
- [10] A. Stathis, A. Ntanos, N. K. Lyras, G. Giannoulis, A. D. Panagopoulos, and H. Avramopoulos, "Toward converged satellite/fiber 1550 nm DS-BB84 QKD networks: Feasibility analysis and system requirements," *Photonics*, vol. 11, no. 7, Article 609, 2024.
- [11] Z. Yang, M. Zolanvari, and R. Jain, "A survey of important issues in quantum computing and communications," *IEEE Communications Surveys & Tutorials*, vol. 25, no. 2, pp. 1059–1094, 2023.